V. T. Rangel-Kuoppa and J. Dekker, Deep levels in GaInAs grown by molecular beam epitaxy and their concentration reduction with annealing treatment, Materials Science and Engineering B 130, 5-10 (2006).

© 2006 Elsevier Science

Reprinted with permission from Elsevier.

ELSEVIER
Materials Science and Engineering B 130 (2006) 5–10
MATERIALS SCIENCE & ENGINEERING B
www.elsevier.com/locate/mseb

Deep levels in GaInAs grown by molecular beam epitaxy and their concentration reduction with annealing treatment

V.T. Rangel-Kuoppa [a,*], J. Dekker [b]

[a] Optoelectronics Research Centre, Tampere University of Technology, P.O. Box 692, 33101 Tampere, Finland
[b] VTT Information Technology, Microelectronics, Tietotie 3, P.O. Box 1208, FIN-02044 VTT, Finland

Received 14 September 2004; received in revised form 7 December 2005; accepted 7 December 2005

Abstract

X-ray diffraction (XRD), current–voltage (*IV*), capacitance–voltage (*CV*), deep-level transient Fourier spectroscopy (DLTFS) and isothermal transient spectroscopy (ITS) techniques are used to investigate the thermal annealing behaviour of three deep levels in $Ga_{0.986}In_{0.014}As$ heavily doped with Si (6.8×10^{17} cm^{-3}) grown by molecular beam epitaxy (MBE). The thermal annealing was performed at 625 °C, 650 °C, 675 °C, 700 °C and 750 °C for 5 min. XRD study shows good structural quality of the samples and yields an In composition of 1.4%. Two main electron traps are detected by DLTFS and ITS around 280 K, with activation energies of 0.58 eV and 0.57 eV, capture cross sections of 9×10^{-15} cm^2 and 8.6×10^{-14} cm^2 and densities of 2.8×10^{16} cm^{-3} and 9.6×10^{15} cm^{-3}, respectively. They appear overlapped and as a single peak, which divides into two smaller peaks after annealing at 625 °C for 5 min.

Annealing at higher temperatures further reduces the trap concentrations. A secondary electron trap is found at 150 K with an activation energy of 0.274 eV, a capture cross section of 8.64×10^{-15} cm^2 and a density of 1.38×10^{15} cm^{-3}. The concentration of this trap level is also decreased by thermal annealing.
© 2005 Elsevier B.V. All rights reserved.

Keywords: Deep level; Molecular beam epitaxy; Annealing; DLTFS; ITS; GaInAs

1. Introduction

GaInAs has been studied extensively in the last years, either lattice matched to InP [1–9] or lattice mismatched on GaAs [10–17]. Due to its infrared sensitivity (∼900–1600 nm) it is a useful material for optical communication, photodiodes, solar cells and laser diodes. These applications have encouraged the study of its electrical, optical and structural characteristics at high In concentrations. Therefore, the available literature for samples with low In contents is typically for samples with the In composition higher than 4.5% [12–15], and only some work [16,17] has been performed with GaInAs having the In composition below 1.2% and grown by molecular beam epitaxy (MBE).

In order to gain better understanding about the nature of the deep levels in GaInAs, samples with low In composition are studied to facilitate the comparison with GaAs results [18,19] in the literature. Although this approach is very similar to the one made by Mircea et al. [15], Ioannu et al. [16] and Bhattacharya et al. [17], the results presented here are very different. Mircea et al. [15] grew their samples by vapour phase epitaxy (VPE) with 4.6% In and a very low doping (2×10^{13} cm^{-3}) finding one single deep centre with an activation energy of 0.78 eV. Ioannu et al. [16] grew their samples by MBE with 0.6% In. They found three deep centres: M1, M3 and M4 according to Lang et al. [19] nomenclature. Their study yielded activation energies (E_A) of 0.21 eV and 0.49 eV for M1 and M4, respectively. Bhattacharya et al. [17] also grew their samples by MBE and found six deep centres [19]: M1, M2, M3, M4, M6 and M7. The results shown here are very different from the former ones. In this paper the presence of the deep level M5 in GaInAs grown by MBE is reported. The presence of a deep level that has not been reported before, with E_A between 0.51 eV and 0.588 eV depending on the thermal annealing treatment, is also reported. A smaller peak with E_A between 0.097 eV and 0.271 eV, also depending on the thermal annealing treatment, is reported. The behaviour of these levels following annealing at a range of temperatures is also discussed.

* Corresponding author. Present address: Optoelectronics Laboratory, Helsinki University of Technology, P.O. Box 3500, Helsinki FIN-02015 HUT, Finland. Tel.: +358 505829122; fax: +358 94513128.
E-mail address: tapio.rangel@hut.fi (V.T. Rangel-Kuoppa).

0921-5107/$ – see front matter © 2005 Elsevier B.V. All rights reserved.
doi:10.1016/j.mseb.2005.12.011

2. Experiment

2.1. Sample growth and preparation

In this paper n-type 2-μm-thick $Ga_{0.986}In_{0.014}As$ heavily doped with Si ($6.8 \times 10^{17}\,cm^{-3}$) grown on an n-type GaAs(1 0 0) substrate by molecular beam epitaxy to GaAs is studied. The samples were cut in pieces before annealing to enable the comparison of as-grown and annealed samples.

The annealing temperatures were 625 °C, 650 °C, 675 °C, 700 °C and 750 °C for 5 min in a thermal annealing (TA) furnace under flowing nitrogen. In order to avoid out-diffusion the samples were capped with 200-nm SiO_2 deposited by plasma enhanced chemical vapour deposition at 300 °C before the thermal treatment.

For the DLTFS study, Schottky contacts were made from 100-nm-thick evaporated Au layer using a lift-off process. The area of the Schottky contact was $5.15 \times 10^{-3}\,cm^2$. An ohmic contact on the backside of the substrate was made by evaporating multiple metal layer structure of 5-nm Ni/5-nm Au/30-nm Ge/100-nm Au, and then annealing the contact for 1 min at 410 °C.

2.2. XRD, IV and CV characterization

X-ray diffraction (XRD) study showed that all the samples had good structural quality and yielded an In composition of 1.4%. The summarized current–voltage (*IV*) and capacitance–voltage (*CV*) results are shown in Table 1.

The voltage bias was −1.5 V. It can be seen that the quality factor of the Schottky contact is highest in the as-grown sample and then improves as the annealing temperature increases. In all cases it is below 2, which is usually considered satisfactory for a reliable Schottky contact. As the annealing temperature increases, saturation currents also increase, showing degradation in the Schottky contact as expected from the degradation of the material due to the annealing. The saturation current is in all cases well below 10 μA and the deep levels are not perturbed by a large leakage current during the reverse bias. Therefore, the depletion regions are really depleted from electrons during the reverse bias. All the *IV* curves showed a correlation value well above 0.99.

The free carrier density calculated from the $1/C^2$ versus V plot does not show large variations with the annealing temperature. The plot showed a very good linearity, with correlation coefficients exceeding 0.999. The *CV* study also yields a depletion region of the order of 100 nm for −0.7 V. The doping profile is practically constant in this region.

Table 1
Current–voltage (*IV*) and capacitance–voltage (*CV*) results for as-grown and annealed samples at room temperature

Annealing temperature (°C)	Quality factor (A)	Saturation current (cm^{-3})	Free carrier density
No	1.919	2.3×10^{-7}	6.83×10^{17}
625	1.418	6.8×10^{-7}	8.94×10^{16}
650	1.739	5.5×10^{-7}	4.12×10^{17}
675	1.795	6.0×10^{-7}	4.09×10^{16}
700	1.671	1.4×10^{-6}	3.84×10^{17}
750	1.537	1.9×10^{-6}	6.74×10^{17}

All the annealing times are 5 min. Voltage bias was −1.5 V.

2.3. DLTFS and ITS characterization

Deep-level transient Fourier spectroscopy (DLTFS) [20] and isothermal transient spectroscopy (ITS) [21] are used to obtain the deep-level density (ρ_{DL}), capture cross section (σ_{DL}) and activation energy (E_A).

The reverse bias used for the DLTFS testing was limited by the low breakdown voltage of the diodes. The breakdown voltage was around −1.7 V. The DLTFS measurements were made using a reverse bias of −0.7 V and a pulse voltage of 0 V. The pulse width was 100 ms and the period width was 100 ms. The pulse width is not included in the period width, and the period width is the same as the emission time window, according to Lang's terminology [22]. The term period width is preferred because it is the one used nowadays. The DLTFS study was done with a BIORAD DL8000 system.

In order to present the data clearly, DLTFS spectra are shown in two figures.

Fig. 1 shows the DLTFS curves and leakage currents for the as-grown sample and the samples annealed at 625 °C, 650 °C and 675 °C. It can be clearly seen from the graphic that the leakage current is well below 10 μA in the temperature range of the DLTFS peaks. This means that thermal equilibrium is kept [22] and the analysis is reliable. Three separate peaks labelled A, B and C can be seen in most of the curves. It can be seen from Fig. 1 that the DLTFS curve of the as-grown sample shows one major peak having an important broadness, and that around 265 K there is a slight shoulder. This could be due to a convolution of two traps. Support for this hypothesis comes after annealing at 625 °C, where the main peak has separated into two smaller peaks, labelled A and B between 250 K and 350 K. It is not clear if the presence of peak B experiences any decrease due to annealing at this temperature, as it

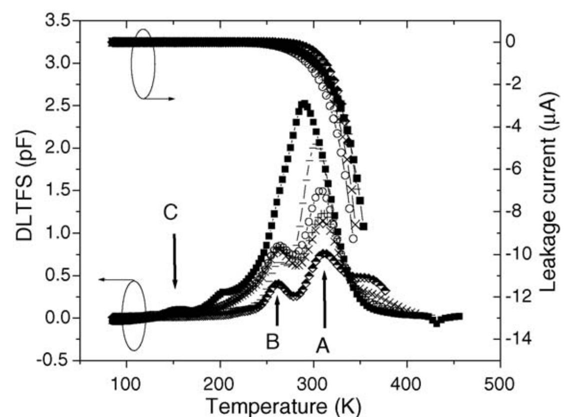

Fig. 1. DLTFS curves and leakage currents of $Ga_{0.986}In_{0.014}As$ Si: doped measured with a pulse width of 100 ms, a period width of 100 ms, a reverse voltage of −0.7 V and a pulse voltage of 0 V. The graphics correspond to the following thermal annealing temperatures: as-grown (■), 625 °C (–), 650 °C (◯) and 675 °C (+). The annealing time was 5 min.

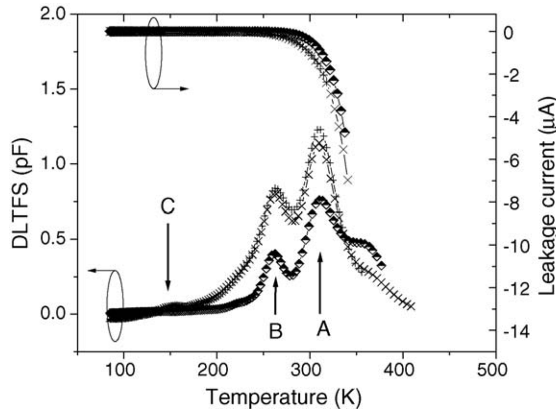

Fig. 2. DLTFS curves and leakage currents of Si-doped $Ga_{0.986}In_{0.014}As$ measured with a pulse width of 100 ms, a period width of 100 ms, a reverse voltage of −0.7 V and a pulse voltage of 0 V. The graphics correspond to the following thermal annealing temperatures: 675 °C (+), 700 °C (×) and 750 °C (⬘). The annealing time was 5 min.

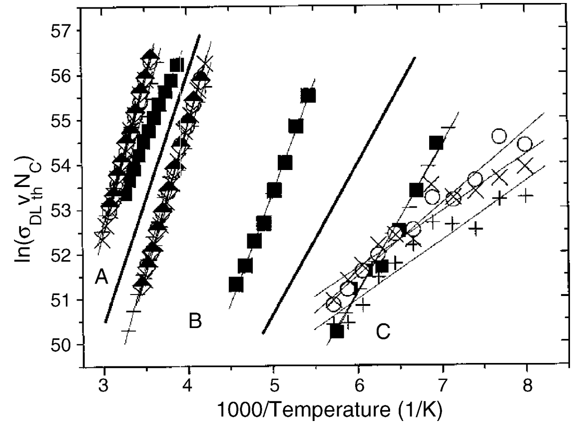

Fig. 4. Arrhenius plot for the DLTFS measurements of traps A, B and C. N_C is the effective density of states, v_{th} is the mean thermal velocity and σ_{DL} is the capture cross section. The graphics correspond to the following thermal annealing temperatures: as-grown (■), 625 °C (−), 650 °C (◯), 675 °C (+), 700 °C (×) and 750 °C (⬘). The annealing time was 5 min. The thick lines are used to separate the respective group of data for each deep level.

could be possible that only peak A decreases. In order to clarify this point subsequent annealing at 650 °C, 675 °C, 700 °C and 750 °C was done. Fig. 2 shows the DLTFS curves and leakage currents for the samples annealed at 675 °C, 700 °C and 750 °C. In Fig. 1 it is possible to see that peak A decreases with increased annealing temperature, while peak B practically remains the same up to annealing temperature of 700 °C (Figs. 1 and 2). Both peaks experience a decrease for annealing at 750 °C.

Another small peak appears approximately at 160 K. The evolution of the peak C with annealing temperature is shown in Fig. 3.

The presence of the peak C decreases with annealing. There is a slight shift to smaller temperatures (meaning smaller activation energies) when annealing at 625 °C but the peak goes back to the same position after annealing at 650 °C (◯), 675 °C (+) and 700 °C. Annealing at 750 °C shifts the position of the peak to the same place as for annealing at 625 °C, but the peak almost disappears. A shoulder appears around 350 K, but it is not reliable due to the high leakage current (around >10 μA). Analysis of this shoulder rendered poor correlation values, below 0.7. One strong candidate for the poor origin of this peak could be the deep level EL2, as it usually appears at this temperature. No further comments can be given, because no reliable activation energy could be obtained due to the high leakage current and poor correlation values.

Fig. 4 shows the Arrhenius plots for all the deep levels and the annealing temperatures. The Arrhenius plots of the as-grown sample for the traps A and B do not overlap as they do for all the annealed samples, in particular for trap B. This is due to the overlapping of the peaks. In order to get an accurate determination of the ρ_{DL}, σ_{DL} and E_A for traps A and B in the as-grown sample, simulation was used. For the simulation, a small program was done that calculates the transients for each deep level, and afterwards the change in capacitance according to the period width.

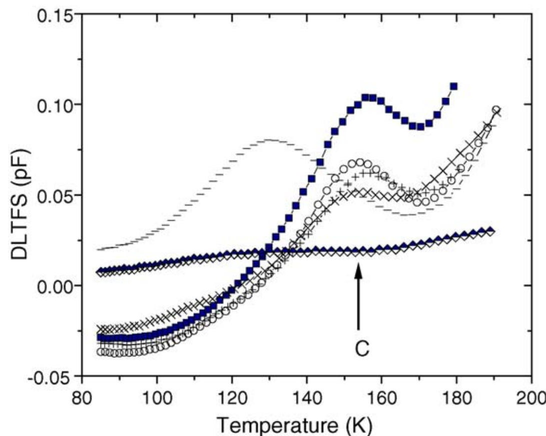

Fig. 3. DLTFS curves for trap C of Si-doped $Ga_{0.986}In_{0.014}As$ measured with a pulse width of 100 ms, a period width of 100 ms, a reverse voltage of –0.7 V and a pulse voltage of 0 V in the range of 80–200 K. The graphics correspond to the following thermal annealing temperatures: as-grown (■), 625 °C (−), 650 °C (◯), 675 °C (+), 700 °C (×) and 750 °C (⬘). The annealing time was 5 min.

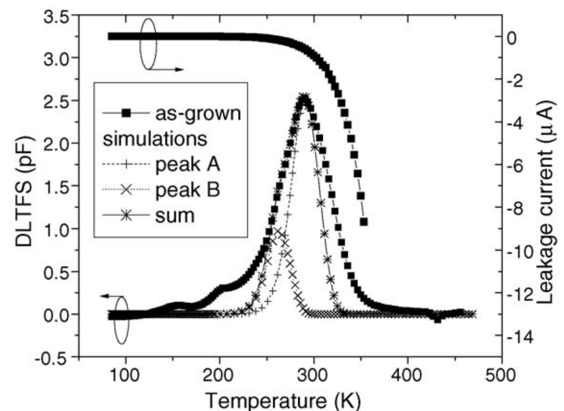

Fig. 5. DLTFS graphics for the as-grown sample, simulations for traps A and B and the sum of both. Also the leakage current is shown for the as-grown sample.

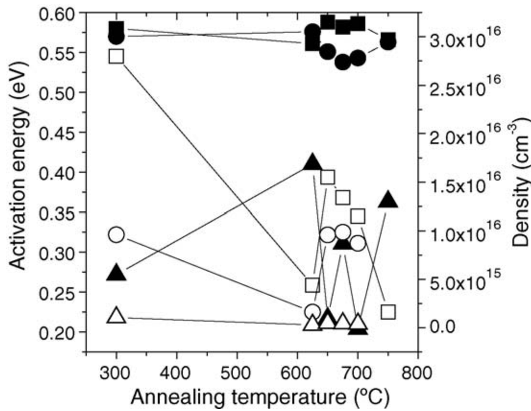

Fig. 6. E_A for deep levels A (■), B (●) and C (▲) and ρ_{DL} for deep levels A (□), B (○) and C (Δ) obtained from the DLTFS Arrhenius plots. The as-grown sample is shown at 300 °C, which is the temperature for SiO_2 deposition.

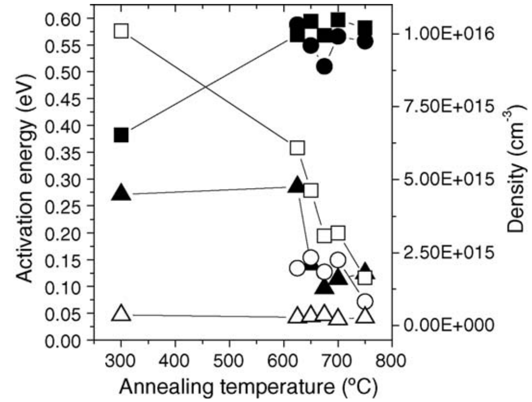

Fig. 8. E_A for deep levels A (■), B (●) and C (▲) and ρ_{DL} for deep levels A (□), B (○) and C (Δ) obtained from the ITS Arrhenius plots. The as-grown sample is shown at 300 °C, which is the temperature for SiO_2 deposition.

In Fig. 5 it is possible to see the DLTFS curve of the as-grown sample and the simulations for the traps A and B. The best simulations were obtained for $E_A = 0.58$ eV and 0.57 eV, $\sigma_{DL} = 9 \times 10^{-15}$ cm^2 and 8.68×10^{-14} cm^2 and $\rho_{DL} = 2.8 \times 10^{16}$ cm^{-3} and 9.6×10^{15} cm^{-3} for the traps A and B, respectively. The broadness of the as-grown sample does not fit totally with the simulation at temperatures above 320 K and below 240 K. This might be due to the high leakage current, which might distort the measurement at higher temperatures and also due to the presence of EL2, as it was discussed before. The accurate values for ρ_{DL}, σ_{DL} and E_A with their precisions and related significant numbers are shown in tables in Appendix A.

Fig. 6 shows the deep-level density and the activation energy for the deep levels A, B and C. The as-grown sample is shown at 300 °C, which is the temperature for SiO_2 deposition.

Isothermal transient spectroscopy [21] study was done for the peaks A, B and C for all the samples, except for the peak B of the as-grown sample due to a serious overlap with the peak A. The ITS measurements were performed starting at 25 K below the peak temperature and finishing at 25 K above the peak temperature. The temperature interval was 5 K, so 11 measurements were done in total for each peak. The peak temperatures were 289 K for peak A, 250 K for peak B and 150 K for peak C. In each scan the period width was varied from 100 μs to 250 ms in geometrical progression with a multiplier of 1.1, i.e., each measuring period width equals 1.1 times the previous measuring period width. Fig. 7 shows the Arrhenius plots for the ITS measurements. It is interesting to note the similarities with Fig. 2. Noteworthy is also the change in the slope for the deep level C for annealing temperatures 650 °C, 675 °C and 700 °C. The slopes do not vary as much as those in the DLTFS measurements.

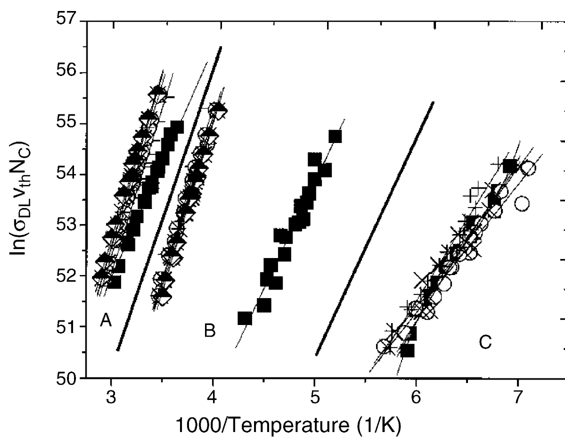

Fig. 7. Arrhenius plot for the ITS measurements of the traps A, B and C. N_C is the effective density of states, v_{th} is the mean thermal velocity and σ_{DL} is the capture cross section. The graphics correspond to the following thermal annealing temperatures: as-grown (■), 625 °C (–), 650 °C (○), 675 °C (+), 700 °C (×) and 750 °C (◆). The annealing time was 5 min. The thick lines are used to separate the respective group of data for each deep level.

Fig. 8 shows ρ_{DL} and E_A obtained by ITS for the deep levels A, B and C. The as-grown sample is shown at 300 °C, which is the temperature for SiO_2 deposition.

3. Results and discussion

The deep levels A and B show an interesting superposition behaviour by forming a single peak for the as-grown sample. This overlap is removed after annealing at 625 °C for 5 min.

Simulation shows that the peak B experiences only a very small change with annealing at 625 °C. Peak B continues showing this behaviour except for annealing at 750 °C. This strongly suggests that peak B might be formed by an impurity, an impurity/point defect or a vacancy. On the other hand, peak A continuously decreases with higher annealing temperatures. This behaviour strongly resembles the behaviour reported by Watson and Ast [14] and Matragano et al. [12] of their peak BC. Watson and Ast [14] report deep level BC to be made up of two peaks, here labelled B′ and C′ to avoid confusion with the nomenclature in this article. The electron trap giving rise to peak B′ is attributed to α misfit dislocations, with an E_A of 0.58 eV. The trap related to the peak C′ in their work was identified as EL2 with E_A equal to 0.73 eV. Clearly, it is not possible to attribute the

same deep centres to the electron traps found in this article due to the difference in E_A for peak C′. Due to the strong similarities in E_A with peak B′, peak A is attributed to α misfit dislocation. This is the level M5 according to the nomenclature of Lang et al. [19].

Bhattacharya et al. [17] used p–n junction in their studies. This led them to attribute this deep level to dislocations in the interface. However, the depletion region studied in our work is of the order of 100 nm, indicating that the deep level arises from the bulk material.

Deep level B has not been reported before in the literature for GaInAs, but it could be related with the level EL4 in GaAs according to Martin et al. [18] nomenclature. EL4 is reported to have an E_A of 0.51 eV and to appear in As rich grown MBE materials, being related with Ga vacancies [17]. Due to the fact that this peak is so similar to peak A in its activation energy and behaviour, it could also be related with misfit dislocations. Further study is necessary to clarify this point.

Deep level C has a very small E_A which is reduced with thermal annealing. It is in the range of the energy for EL10 [18] and M1 [19], which appear under As rich growth conditions. However, ρ_{DL} stays almost invariant, decreasing just slightly. This strongly suggests that the deep level is related to a point defect/impurity complex.

4. Summary

As-grown and annealed samples of $Ga_{0.986}In_{0.014}As$ heavily doped with Si (6.8×10^{17} cm^{-3}) and lattice mismatched with GaAs have been studied by XRD, *IV*, *CV*, DLTFS and ITS techniques. The annealing temperatures were 625 °C, 650 °C, 675 °C, 700 °C or 750 °C, all for 5 min. XRD results show good crystal quality and 1.4% In composition for all the samples. *IV* and *CV* studies confirm that the Schottky contacts are satisfactory. The doping profile is practically constant up to 100 nm inside the material. The correlation factors are always above 0.99. DLTFS and ITS studies show the presence of three clear peaks, with activation energies of 0.58 eV, 0.55 eV and 0.27 eV. The main peak in the as-grown sample turns out to be a convolution of two peaks, labelled A and B, confirmed by simulations. The peaks can be seen separated after annealing at 625 °C for 5 min. Annealing decreases the height of peak A only, not affecting peak B. Annealing at higher temperatures affects only peak A, leaving almost invariant peak B up to annealing at 750 °C, when both peaks suddenly drop. This behaviour and comparison with the literature strongly suggest that peak A is related to M5 deep centre caused by α misfit dislocations. Peak B strongly resembles deep level EL4, which is related to As rich material and caused by point defects or point defect/impurity complexes. Due to its very similar activation energy and behaviour to peak A, it could also be related with dislocations. Further study is necessary to clarify this point. Peak C is attributed to deep centres EL10 and M1, and due to its density invariance with annealing it is presumed to be related with a point defect/impurity.

Acknowledgements

The authors are grateful to S. Karirinne, T. Jouhti and J. Kontinen for growing the samples. Special gratitude is expressed to H. Lipsanen and M. Sopanen for their scientific opinion. This work was supported, in part, by the Academy of Finland within the framework of the DIODE Project and by the National Council for Science and Technology (CONACYT) of Mexico, Fellowship 136605.

Appendix A

A.1. DLTFS calculated parameters via Arrhenius plot

A.1.1. Trap A

Annealing temperature (°C)	Activation energy (E_A) (eV)	Capture cross section (σ_{DL}) (cm^2)	Density (ρ_{DL}) (cm^{-3})	Correlation
As-grown	0.41	4.4×10^{-17}	$3. \times 10^{16}$	0.99572
As-grown (simulation)	0.58	9×10^{-15}	2.8×10^{16}	
625	0.56	7.3×10^{-15}	4.4×10^{15}	0.9985
650	0.58	1.3×10^{-14}	1.5×10^{16}	0.99929
675	0.58	9.1×10^{-15}	1.3×10^{16}	0.9992
700	0.58	1×10^{-14}	1.1×10^{16}	0.99934
750	0.56	4.5×10^{-15}	1.6×10^{15}	0.9971

The maximum errors for E_A, σ_{DL} and ρ_{DL} are 2.3%, 7.8% and 9.1%, respectively.

A.1.2. Trap B

Annealing temperature (°C)	Activation energy (E_A) (eV)	Capture cross section (σ_{DL}) (cm^2)	Density (ρ_{DL}) (cm^{-3})	Correlation
As-grown	0.38	1.3×10^{-14}	3.8×10^{15}	0.98306
As-grown (simulation)	0.57	8.7×10^{-14}	9.6×10^{15}	
625	0.57	4×10^{-13}	1.6×10^{15}	0.98304
650	0.55	1.5×10^{-13}	9.6×10^{15}	0.99435
675	0.54	8.7×10^{-14}	9.8×10^{15}	0.99737
700	0.54	1.2×10^{-13}	8.7×10^{15}	0.99792
750	0.56	2.9×10^{-13}	9×10^{14}	0.99833

The maximum errors for E_A, σ_{DL} and ρ_{DL} are 3.1%, 7.2% and 9.7%, respectively.

A.1.3. Trap C

Annealing temperature (°C)	Activation energy (E_A) (eV)	Capture cross section (σ_{DL}) (cm^2)	Density (ρ_{DL}) (cm^{-3})	Correlation
As-grown	0.27	9.1×10^{-15}	1×10^{15}	0.98032
625	0.41	1.6×10^{-13}	2.8×10^{14}	0.98617
650	0.22	1.9×10^{-16}	4.8×10^{14}	0.98231
675	0.31	1.3×10^{-13}	4.4×10^{14}	0.98179
700	0.2	5.3×10^{-17}	3.9×10^{14}	0.93373
750	0.36	7×10^{-16}	1.9×10^{14}	0.95645

The maximum errors for E_A, σ_{DL} and ρ_{DL} are 2%, 7.2% and 8.7%, respectively.

A.2. ITS calculated parameters via Arrhenius plot

A.2.1. Trap A

Annealing temperature (°C)	Activation energy (E_A) (eV)	Capture cross section (σ_{DL}) (cm^2)	Density (ρ_{DL}) (cm^{-3})	Correlation
As-grown	0.38	1.2×10^{-17}	1×10^{16}	0.99843
625	0.57	1×10^{-14}	6×10^{15}	0.99977
650	0.59	1.7×10^{-14}	4.6×10^{15}	0.99974
675	0.57	5.2×10^{-15}	3×10^{15}	0.99988
700	0.59	1.7×10^{-14}	3.2×10^{15}	0.9999
750	0.58	9.4×10^{-15}	1.6×10^{15}	0.99995

The maximum errors for E_A, σ_{DL} and ρ_{DL} are 2.4%, 7.9% and 8.9%, respectively.

A.2.2. Trap B

Annealing temperature (°C)	Activation energy (E_A) (eV)	Capture cross section (σ_{DL}) (cm^2)	Density (ρ_{DL}) (cm^{-3})	Correlation
625	0.59	7.6×10^{-13}	2×10^{15}	0.99945
650	0.55	1.8×10^{-13}	2.3×10^{15}	0.99949
675	0.51	4×10^{-14}	1.8×10^{15}	0.99935
700	0.57	4.2×10^{-13}	2.2×10^{15}	0.99802
750	0.56	2.5×10^{-13}	8.2×10^{14}	0.9997

The maximum errors for E_A, σ_{DL} and ρ_{DL} are 2.1%, 7.3% and 9.1%, respectively.

A.2.3. Trap C

Annealing temperature (°C)	Activation energy (E_A) (eV)	Capture cross section (σ_{DL}) (cm^2)	Density (ρ_{DL}) (cm^{-3})	Correlation
As-grown	0.27	8.9×10^{-15}	3.6×10^{14}	0.98616
625	0.28	2.7×10^{-14}	2.8×10^{14}	0.99897
650	0.14	8.1×10^{-19}	3.2×10^{14}	0.98468
675	0.1	6.4×10^{-20}	3.6×10^{14}	0.97894
700	0.11	1×10^{-19}	2.2×10^{14}	0.96122
750	0.12	3.1×10^{-19}	2.7×10^{14}	0.96534

The maximum errors for E_A, σ_{DL} and ρ_{DL} are 1.9%, 6.8% and 8.7%, respectively.

References

[1] Y. Takanashi, N. Kondo, J. Appl. Phys. 85 (1999) 633.
[2] W. Gao, P. Berger, M. Ervin, J. Pamulapati, R. Lareau, S. Schauer, J. Appl. Phys. 80 (1996) 7094.
[3] B. Srocka, H. Scheffler, D. Bimberg, Appl. Phys. Lett. 64 (1994) 2679.
[4] G.J. Shaw, R.J. Walters, S.R. Messenger, G.P. Summers, J. Appl. Phys. 74 (1993) 1629.
[5] G.J. Shaw, S.R. Messenger, R.J. Walters, G.P. Summers, J. Appl. Phys. 73 (1993) 7244.
[6] W.-P. Hong, C. Canneau, J.R. Hayes, R. Bhat, G.K. Chang, C. Nguyen, Y.H. Jeong, S. Hadjipanteli, A.A. Illiadias, J. Appl. Phys. 70 (1991) 502.
[7] M. Kondow, K. Uomi, A. Niwa, T. Kitatani, S. Watahiki, Y. Yazawa, Solid State Device Materials, Osaka, 1995, p. 1016.
[8] M. Kondow, K. Uomi, A. Niwa, T. Kitatani, S. Watahiki, Y. Yazawa, Jpn. J. Appl. Phys. 35 (1996) 1273.
[9] A.Y. Polyakov, N.B. Smirnov, A.V. Govorkov, A.E. Botchkarev, N.N. Nelson, M.M.E. Fahmi, J.A. Griffin, A. Khan, S.N. Mohammad, D.K. Johnstone, V.T. Bublik, K.D. Chsherbatchev, M.I. Voronova, V.S. Kasatochkin, Solid-State Electron. 46 (2002) 2155.
[10] A. Du, M. Li, T. Chong, K. Teo, W. Lau, Z. Zhang, Appl. Phys. Lett. 69 (1996) 2849.
[11] Y. Uchida, H. Kakibayashi, S. Goto, J. Appl. Phys. 74 (1993) 6720.
[12] M. Matragrano, G. Watson, D. Ast, T. Anderson, B. Pathangey, Appl. Phys. Lett. 62 (1993) 1417.
[13] A. Irvine, D. Palmer, Phys. Rev. Lett. 68 (1992) 2168.
[14] G. Watson, D. Ast, J. Appl. Phys. 71 (1992) 3399.
[15] A. Mircea, A. Mitonneau, J. Hallais, Phys. Rev. B 16 (1977) 3665.
[16] D. Ioannou, Y. Huang, A. Iliadis, Appl. Phys. Lett. 52 (1988) 2258.
[17] P. Bhattacharya, S. Dhar, P. Berger, F.-Y. Juang, Appl. Phys. Lett. 49 (1986) 470.
[18] G.M. Martin, A. Mitonneau, A. Mircea, Electron. Lett. 13 (1977) 191.
[19] D. Lang, A. Cho, A. Gossard, M. Ilegems, W. Wiegmann, J. Appl. Phys. 47 (1976) 2558.
[20] S. Weiss, R. Kassing, Solid-State Electron. 31 (1988) 1733.
[21] J. Samitier, J.R. Morante, A. Cornet, A. Herms, P. Roura, A. Pérez, Mater. Sci. Forum 10–12 (1986) 539.
[22] D.V. Lang, J. Appl. Phys. 45 (1974) 3023.